CO_2-cAMP-Responsive cis-Elements Targeted by a Transcription Factor with CREB/ATF-Like Basic Zipper Domain in the Marine Diatom *Phaeodactylum tricornutum*[1][W][OA]

Naoki Ohno, Takuya Inoue, Ryosuke Yamashiki, Kensuke Nakajima, Yuhei Kitahara, Mikiko Ishibashi, and Yusuke Matsuda*

Research Center for Environmental Bioscience, Department of Bioscience, Kwansei-Gakuin University, Sanda, Hyogo 669–1337, Japan

Expression controls of the carbon acquisition system in marine diatoms in response to environmental factors are an essential issue to understand the changes in marine primary productivity. A pyrenoidal β-carbonic anhydrase, PtCA1, is one of the most important candidates to investigate the control mechanisms of the CO_2 acquisition system in the marine diatom *Phaeodactylum tricornutum*. A detailed functional assay was carried out on the putative core regulatory region of the *ptca1* promoter using a β-glucuronidase reporter in *P. tricornutum* cells under changing CO_2 conditions. A set of loss-of-function assays led to the identification of three CO_2-responsive elements, TGACGT, ACGTCA, and TGACGC, at a region −86 to −42 relative to the transcription start site. Treatment with a cyclic (c)AMP analog, dibutyryl cAMP, revealed these three elements to be under the control of cAMP; thus, we designated them, from 5′ to 3′, as CO_2-cAMP-Responsive Element1 (CCRE1), CCRE2, and CCRE3. Because the sequence TGACGT is known to be a typical target of human Activating Transcription Factor6 (ATF6), we searched for genes containing a basic zipper (bZIP) region homologous to that of ATF6 in the genome of *P. tricornutum*. Gel-shift assays using CCRE pentamers as labeled probes showed that at least one candidate of bZIP proteins, PtbZIP11, bound specifically to CCREs. A series of gain-of-function assays with CCREs fused to a minimal promoter strongly suggested that the alternative combination of CCRE1/2 or CCRE2/3 at proper distances from the minimal promoter is required as a potential target of PtbZIP11 for an effective CO_2 response of the *ptca1* gene.

Marine diatoms are the most successful group of algae in the ocean and are responsible for about one-fifth of global carbon fixation (Tréguer et al., 1995; Falkowski et al., 2000). The maximum CO_2 concentration dissolved in seawater under the present atmosphere at 20°C is calculated to be below 15 μM, which is far lower than the $K_m[CO_2]$ of the carbon fixation enzyme Rubisco in diatoms (Badger et al., 1998). This implies that CO_2 in seawater would not support sufficient primary production; instead, an alternative inorganic carbon source is additionally required for it. It has been well established that many microalgae including marine diatoms possess CO_2-concentrating mechanisms (CCMs), which actively take up both CO_2 and HCO_3^- from the surrounding media and efficiently supply CO_2 from accumulated HCO_3^- to Rubisco (Kaplan et al., 1980; Colman and Rotatore, 1995; Matsuda and Colman, 1995; Johnston and Raven, 1996; Matsuda et al., 2001; Moroney and Ynalvez, 2007; Spalding, 2008; Trimborn et al., 2008). Besides the CCMs, it has been reported in one species of marine diatom that a C_4-like metabolism also operates in the CO_2 acquisition system (Reinfelder et al., 2004). However, general occurrences of a C_4-type system in diatoms are still in question (Roberts et al., 2007; Matsuda et al., 2011).

The activity of CCMs is suppressed under high-CO_2 conditions and induced (or derepressed) under normal air (and/or further lower CO_2) conditions in a few hours (Kaplan et al., 1980; Miller et al., 1990; Colman and Rotatore, 1995; Matsuda and Colman, 1995; Johnston and Raven, 1996; Matsuda et al., 2001; Kucho et al., 2003; Vance and Spalding, 2005). This indicates that algal cells can perceive changes in ambient CO_2 concentration as a signal and acclimate to new CO_2 conditions in a short period. Mechanisms of acclimation to CO_2 and its relationship with other abiotic signals in major oceanic primary producers such as diatoms are a critical matter in order to understand the

[1] This work was supported by the Ministry of Education, Culture, Sports, Science and Technology of Japan (to Kwansei Gakuin University) and by the Steel Industry Foundation for the Advancement of Environmental Protection Technology (to Y.M.).

* Corresponding author; e-mail yusuke@kwansei.ac.jp.

The author responsible for distribution of materials integral to the findings presented in this article in accordance with the policy described in the Instructions for Authors (www.plantphysiol.org) is: Yusuke Matsuda (yusuke@kwansei.ac.jp).

[W] The online version of this article contains Web-only data.

[OA] Open Access articles can be viewed online without a subscription.

www.plantphysiol.org/cgi/doi/10.1104/pp.111.190249

fate of aquatic primary productivity. Notwithstanding, molecular level studies of them are still in their infancy.

In contrast, mechanisms of CCM regulation by CO_2 have been well studied in cyanobacteria. In *Synechocystis* sp. PCC 6803, the *cytoplasmic-membrane protein* (*cmp*) *ABCD* operon, which encodes Bicarbonate Transporter1, is induced by binding of Cytoplasmic-membrane protein Regulator (CmpR) to the promoter under low-CO_2 conditions (Omata et al., 2001; Nishimura et al., 2008), but in contrast to this, other CO_2-responsive genes (e.g. *sodium bicarbonate transporter* (*sbt*)*A/sbtB*, *NAD(P)H dehydrogenase* (*ndh*)*F3/ndhD3/*CO_2 *hydration protein Y/open reading frame133*, and *modified NDH-1* (*mnh*)*D1/mnhD2*) are repressed by binding of CO_2-concentrating mechanism Regulator (CcmR)/NAD(P)H dehydrogenase Regulator (NdhR) to their promoters under high-CO_2 conditions (Wang et al., 2004; Price et al., 2008). Similar functions of CcmR/NdhR were also observed in the marine cyanobacterium *Synechococcus* sp. PCC7002 (Price et al., 2008).

On the other hand, knowledge about the regulations of putative CCM components is relatively limited in eukaryotic algae. In the green alga *Chlamydomonas reinhardtii*, it is known that the transcriptional regulation of a periplasmic carbonic anhydrase (CA), *Cah1* (Fujiwara et al., 1990), and mitochondrial CA, mtCA, are highly responsive to ambient CO_2 concentration (Eriksson et al., 1998). The transcriptional activity of a promoter region of *Cah1* is known to be under bidirectional controls in response to CO_2, being ensured by enhancer and silencer regions, which reside back to back on the *Cah1* promoter. This enhancer region is further found to possess two critical elements designated as enhancer-element consensus (Kucho et al., 2003), which is the target of a class of transcription factors, enhancer-element consensus-binding proteins (Yoshioka et al., 2004). Although the upstream signal cascade toward this promoter is not known in *C. reinhardtii*, a zinc finger protein, CCM1/Cia5, has been found to govern the up-regulation of most low-CO_2-inducible genes and thus is considered to be a master regulator of the transcriptional response (Fukuzawa et al., 2001; Xiang et al., 2001).

The CCM and controls on expression of the genes involved in response to changes in ambient [CO_2] are also observed in many marine eukaryotic photoautotrophs (Johnston and Raven, 1996; Badger et al., 1998; Sültemeyer 1998; Thoms et al., 2001; Matsuda et al., 2001; Colman et al., 2002). In marine diatoms, physiological evidence has shown that active uptake systems for CO_2 and HCO_3^- operate in both centric and pennate species (Rotatore and Colman, 1992; Burkhardt et al., 2001; Matsuda et al., 2001, 2011; Chen et al., 2006; Trimborn et al., 2008). Since both the capacity to take up dissolved inorganic carbon (DIC) and a cell's affinity for DIC were shown to be induced upon transferring cells of the marine diatom *Phaeodactylum tricornutum* from high CO_2 to air (Matsuda et al., 2001), DIC uptake and internal CO_2 flow toward Rubisco seem to be strengthened under CO_2 limitation. As one of the putative key components for this acclimation process, chloroplastic CAs have been isolated and genes have been cloned (Satoh et al., 2001; Harada and Matsuda, 2005).

Similarly to CCMs in green algae and cyanobacteria, CAs at close proximity to Rubisco must play a crucial role in marine diatoms to create an efficient flux of CO_2 to Rubisco under CO_2-limiting conditions. Two β-type CAs, PtCA1 and PtCA2, found as chloroplast-localized enzymes in *P. tricornutum*, were localized in the pyrenoid, a large protein body in the stroma, and it is known that the C-terminal amphipathic helices of PtCAs play a role in the formation of a protein complex in the pyrenoid (Tanaka et al., 2005; Kitao and Matsuda, 2009; Tachibana et al., 2011). Transcription of the *ptca1* and *ptca2* genes is regulated by CO_2, and the response of *ptca1* to changes in [CO_2] has been shown to be stronger than that of *ptca2* (Harada et al., 2005, 2006).

The function of PtCA1 has yet to be determined, but this enzyme is one of the most interesting candidates for elucidating the molecular mechanisms of the CCM and acclimation to CO_2 in diatoms. In previous studies, the promoter region of *ptca1* (P*ptca1*) was isolated, and it was shown that the core regulatory region is composed of two putative cAMP-response elements (CRE1 and CRE2) and a putative p300-binding element (p300be; Harada et al., 2006); additionally, a putative SKiNhead-1 (Skn-1)-binding element was found downstream of the p300be (in this article). CRE and p300be were related to cAMP response elements in mammalian systems (Montminy et al., 1986; Deutsch et al., 1988; Rikitake and Moran 1992; Tanaka et al., 1997), and Skn-1 was activated by binding with cAMP-responsive element-binding protein 1 in the nematode *Caenorhabditis elegans* (Walker et al., 2000). It was indeed shown in *P. tricornutum* that transcription of *ptca1* was repressed even under CO_2-limiting conditions in the presence of the cAMP analog, dibutyryl cAMP (dbcAMP; Harada et al., 2006). This repressive effect of dbcAMP was negated by impairing the sequences around CREs and p300be (Harada et al., 2006), thus strongly suggesting that the core regulatory region of P*ptca1* is under the repressive control of cAMP as a second messenger for CO_2 signaling, but critical cis-elements for this process have yet to be determined in the P*ptca1* promoter.

The perception of CO_2 signals via cAMP has been reported in cyanobacteria, a pathogenic fungus, and mammals. The activity of soluble adenylyl cyclase (sAC) in rat testis is regulated by HCO_3^- and pH, and it functions as a HCO_3^- sensor (Chen et al., 2000). In the pathogenic fungus *Candida albicans*, the activity of sAC was related directly to the regulation of filamentation by CO_2/HCO_3^- (Klengel et al., 2005). The activity of CyaB1, one of the sACs in *Anabaena* PCC7120, is also regulated by HCO_3^- (Cann et al., 2003). In the cyanobacterium *Synechocystis* PCC6803, it was shown that another sAC, Cya1, is regulated directly by CO_2 rather than HCO_3^- (Hammer et al., 2006). However, there are no data yet to support the relationship between sACs and CCM regulation in cyanobacteria, while it is strongly suggested that a product of the

photorespiratory pathway, 2-phosphoglycolate, directly enhances the binding of CmpR to the promoter of the *cmpABCD* operon to ensure the CO_2 response of this promoter (Nishimura et al., 2008). In eukaryotic algae, besides the above-described information from *C. reinhardtii* and *P. tricornutum*, little is known about the sensing mechanism for ambient CO_2 concentrations, the subsequent signal transduction pathways, and transcriptional controls of promoters in response to changes in CO_2 concentration.

In this study, critical cis-elements required for the CO_2-cAMP response of the *ptca1* promoter were identified, and transcription factors that may target the responsive elements were investigated.

RESULTS

Determination of Critical CO_2-Responsive Elements in the Core Regulatory Region of P*ptca1*

Our previous study has shown that the core regulatory region governing the CO_2 response of P*ptca1* resided −80 bp downstream relative to the transcription start site. To determine the precise CO_2-responsive elements of P*ptca1*, a linker scan and the following one-base replacement assays were carried out on this core region. A series of linker-scan substitutions by the *Not*I restriction site (Fig. 1A) were introduced into the putative core regulatory region (−80 to +61 relative to the transcription start site) of P*ptca1* (Fig. 1B). These fragments were ligated to the β-glucuronidase gene, *uidA*, and were transformed into *P. tricornutum* by microparticle bombardment. As shown in the previous study (Harada and Matsuda, 2005), transcript levels of *uidA* closely reflected the levels of GUS activity in *P. tricornutum*. The results in Figure 2 show the apparent loss of the CO_2 response in the manipulated promoters LS1 to LS3 and LS5 to LS7. In contrast, other linker-scan promoters exhibited a clear CO_2 response equivalent to that observed in the intact promoter (Fig. 2, LS-). Since the impaired sites of LS1 to LS3 and LS5 to LS7 corresponded, respectively, to regions around CRE1 and p300be, it was likely that these two elements are required for the CO_2 response, as was assumed previously (Harada et al., 2005), while other sequences including the Skn-1 and the CRE2 elements were not required for the CO_2 response of P*ptca1*. Levels of GUS activities expressed in transformants varied significantly depending upon clones. This is presumably due to position effects and the copy number of the promoter::*uidA* constructs integrating into different parts of the genome. However, GUS activity ratios (air to 5% CO_2) were relatively stable, which enabled us to assess the CO_2 response with some accuracy (Fig. 2). GUS activity ratios are thus presented for the GUS promoter assays hereafter.

We followed these initial results by determining the precise CO_2-responsive elements around the putative CRE1 and p300be elements. Single-nucleotide exchanges within purines or pyrimidines (A for C or T for G and vice versa) in regions around CRE1 (Fig. 3A) and p300be (Fig. 3B) revealed that the sequences 5′-ACGTCA-3′ (−68 to −63) and 5′-GTGACGC-3′ (−47 to −41), which did not completely overlap with CRE1 and p300be, were critical for the CO_2 response (Fig. 3). This implied that the originally described CO_2-responsive elements, CRE1 and p300be, were not adequately defined. Raw activity data for Figure 3 are available in Supplemental Figure S4.

Search for Further Upstream Elements That May Work Cooperatively with Elements around CRE1 and p300be

The intact promoter, which has both ACGTCA and GTGACGC motifs, showed a clear CO_2 response (Fig. 4A, i). On the other hand, impairment of either one or both of these motifs by *Not*I insertion resulted in the loss of CO_2 response (Fig. 4A, ii–iv). Interestingly, however, addition of the upstream sequence of P*ptca1* (−1,292 to −81) to the region upstream of the short promoter sequence (−80 to +61), in which one of two critical CO_2-responsive motifs was impaired by the *Not*I insertion, conferred a clear CO_2 response on P*ptca1* (Fig. 4A, vi and vii). However, such synergistic effects on the CO_2 response did not occur when both of these motifs were impaired by *Not*I insertion (Fig. 4A, viii). These results indicated the occurrence of additional critical elements upstream of −80 relative to the transcription start site, which could work cooperatively with the two newly found motifs.

In order to detect the upstream elements, which were anticipated from the results of Figure 4A to work cooperatively with the two elements, the long P*ptca1* constructs with singly mutated motifs (Fig. 4A, vi and vii) were truncated from upstream at positions −484, −225, −115, and −80 relative to the transcription start site and promoter activity was compared with those of intact promoters of each length (Fig. 4B). All transformants with these truncated constructs exhibited a clear CO_2 response, with GUS activity ratios between 1.8 and 7.0 (Fig. 4B, ii, iii, v, vi, viii, and ix), except that *uidA* was totally derepressed when truncations were made to −80 (Fig. 4A, xi and xii). Results of GUS assays on cells containing the intact promoters of each length are also shown as controls (Fig. 4B, i, iv, vii, and x). These results clearly demonstrated the occurrence of the additional CO_2-responsive element, which works with either of two downstream elements, at the region −115 to −80 relative to the transcription start site of P*ptca1*. Raw activity data for Figure 4 are available in Supplemental Figure S4.

Role of Three Inverted Sequences, 5′-TGACGT/C-3′ in Responsiveness to CO_2 and cAMP

The primary sequence between −115 and −80 relative to the transcription start site revealed a specific motif sequence at −86 to −81 (Fig. 5A). This sequence, 5′-TGACGT-3′, was highly homologous to one of the

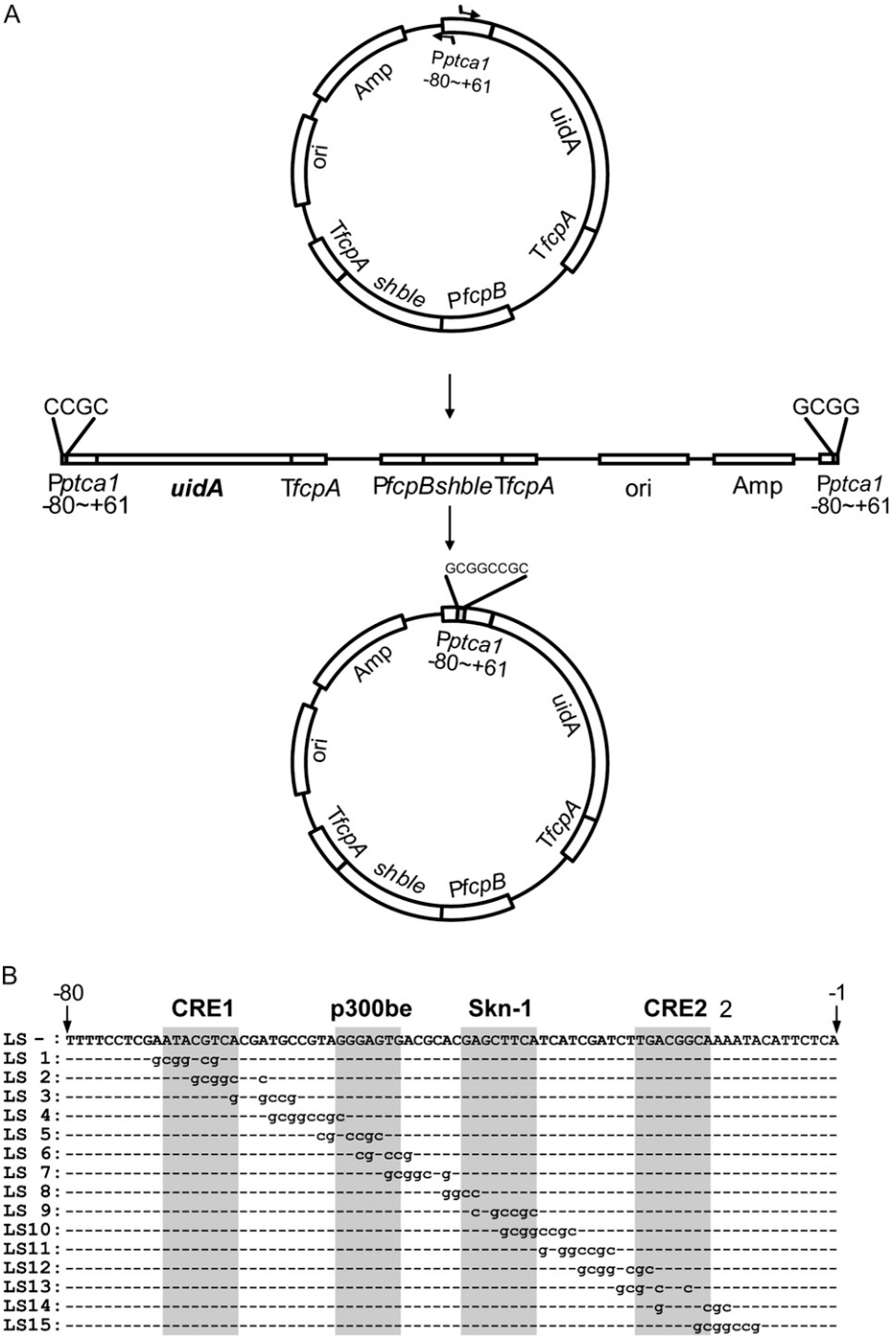

Figure 1. Linker-scan constructs. A, The promoter region of *ptca1* from −80 to +61 relative to the transcription start site was packaged into the transformation vector pPha-T1 upstream of the GUS reporter gene *uidA*. The *Not*I restriction site (gcggccgc) was introduced between −71 and −8 relative to the transcription start site by inverse PCR on pPha-T1 with P*ptca1* (−80 to +61) as the template. The resulting PCR products were self-ligated. B, The position of the introduced *Not*I site was slid toward downstream by 4 bp from LS1 to LS15. CRE1 and CRE2, p300be, and a putative Skn-1 site are indicated at the top of the sequence and highlighted in gray.

critical elements, 5′-TGACGC-3′, at −47 to −42 (Fig. 5A). These two motifs are of complementary relationship with the other critical element, 5′-ACGTCA-3′, at −68 to −63 (Fig. 5A). When either the −86 to −81 or the −47 to −42 sequence relative to the transcription start site was replaced by the *Not*I sequence, the CO_2 response of the promoter (−90 to +61) was well conserved (Fig. 5B, ii and iv). Furthermore, treatment with dbcAMP repressed these mutated promoters even under the air condition, mimicking the response under 5% CO_2 (Fig. 5B, ii and iv). However, impairment of the −68 to −63 sequence relative to the transcription start site or impairments of more than two motifs of these three inverted sequences resulted in full derepression of these manipulated promoters under 5% CO_2 (Fig. 5B, iii and v–viii). dbcAMP treatment also became completely ineffective in regulating these manipulated promoters; that is, the *uidA* reporter was derepressed independently of either CO_2 or dbcAMP (Fig. 5B, iii and v–viii). According to these

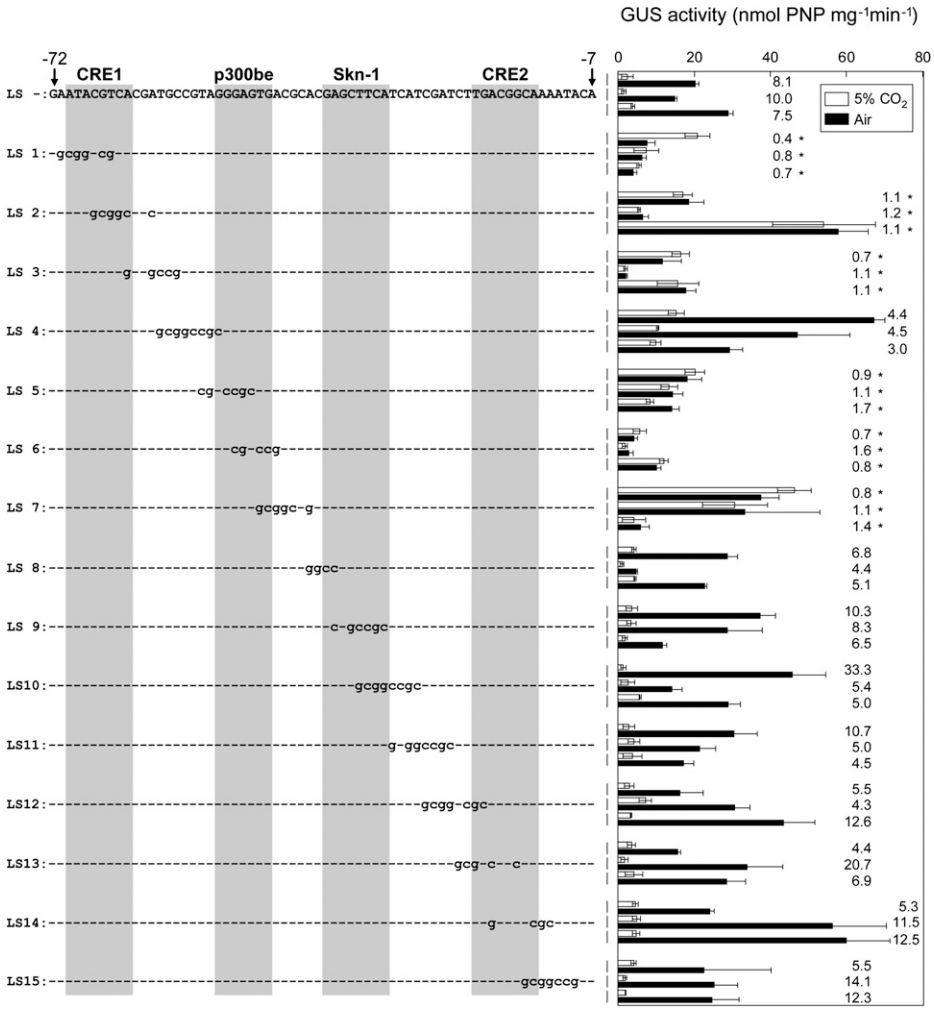

Figure 2. GUS reporter assay of *P. tricornutum* cells transformed with intact P*ptca1* and the linker-scan constructs. Schematic drawings of native P*ptca1* (−80 to +61; LS-) and the linker-scan constructs 1 to 15 (LS1–LS15) are indicated at the left. GUS activity per total protein in lysates was determined in three clones of each transformant grown in 5% CO_2 (white bars) or air (black bars). Values of each bar are means ± SD from three separate cultures. Ratios of GUS activity in air-grown cells to that in 5% CO_2-grown cells are shown to the right of the bars. Asterisks indicate ratios below 2.0. PNP, *p*-Nitrophenol.

results, three inverted elements were designated, from 5′ to 3′, as CO_2-cAMP-Responsive Element1 (CCRE1), CCRE2, and CCRE3 (Fig. 5A), and it was strongly suggested that CCRE2 is the most important element for the CO_2-cAMP response, as a single impairment of this sequence totally abolished the function of P*ptca1* (Fig. 5B, iii). Raw activity data for Figure 5 are available in Supplemental Figure S4.

Search for Putative Transcription Factors That May Target CCREs

The CCRE1 element was identical to the cis-element known to be the typical target sequence of human Activating Transcription Factor6 (ATF6; Wang et al., 2000). This prompted us to search for homologs of human ATF6 in the genome database of *P. tricornutum*. Candidates were screened on the basis of homology of the DNA-binding site, NxxSAxxSR, which is well conserved in the mammalian ATF6 family (Vinson et al., 2002), and the putative Leu-zipper motif, whose primary structure is constituted of a heptad repeat of Leu residues (Fig. 6A). As a result, eight genes were found as candidates encoding basic zipper (bZIP) proteins that may target CCREs in P*ptca1* (Fig. 6A). Seven of these bZIP sequences, PtbZIP7, -8, -11, -12, -13, -15, and -16, were recently described and grouped by Rayko et al. (2010), although PtbZIPx had not previously been reported. The critical amino acid sequence for the bZIP domain deduced from these eight genes revealed significant similarity (Fig. 6A), although the sequence similarity of other regions of the open reading frames of these putative proteins was minimal (Supplemental Fig. S1). These eight candidates were expressed in *Escherichia coli* BL21(DE3), and PtbZIP11, -15, and -16 were successfully expressed as soluble proteins, whereas the other candidates were found in insoluble fractions (Supplemental Fig. S2). For PtbZIP13, we could not detect induction in the *E. coli* system (Supplemental Fig. S2), so it was not studied further.

Gel-Shift Assay of the CCRE Sequences by PtbZIP11, -15, and -16

PtbZIP11, -15, and -16 were purified by nickel-Sepharose column chromatography (Supplemental Fig. S3), and the binding capacity of these candidates

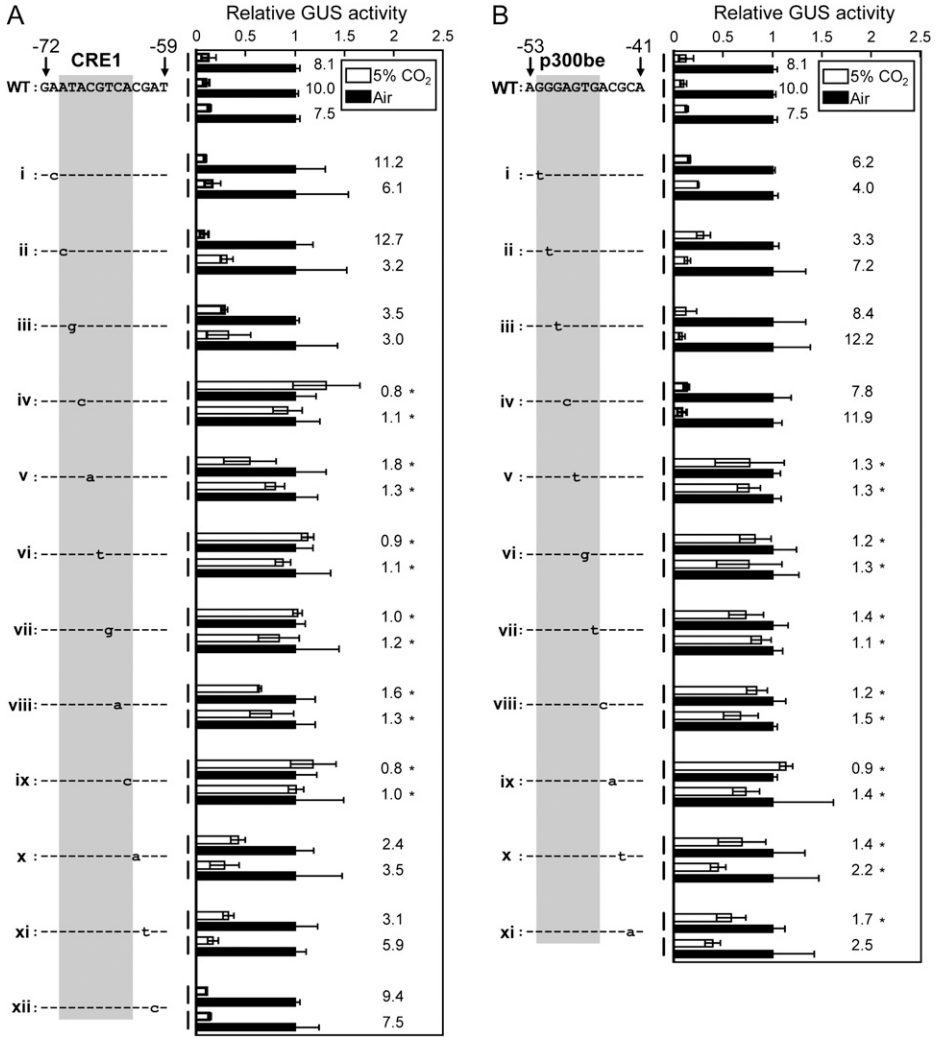

Figure 3. One-base replacements introduced to regions around the putative CRE1 and putative p300be elements, and effects on GUS activity. A, One-base replacements introduced to regions around CRE1 (−71 to −60) are shown in the left half. GUS reporter assays performed on transformants with each construct of P*ptca1*::*uidA* are shown in the right half. B, One-base replacements introduced to regions around p300be (−52 to −42) are shown in the left half. GUS reporter assays done on transformants with each construct of P*ptca1*::*uidA* are shown in the right half. GUS activities in lysates of each transformant grown in 5% CO_2 (white bars) are expressed as relative values to those in air-grown cells (black bars). GUS reporter assays were performed on two to three clones obtained from each transformant. Values of each bar are means ± SD obtained from three separate cultures. Ratios of GUS activity in air-grown cells to that in 5% CO_2-grown cells are shown to the right of the bars. Asterisks indicate ratios below 2.0.

to a pentameric repeat of the TGACGT motif, $(TGACGT)^5$, was examined. When 5 to 75 μg mL^{-1} PtbZIP15 and -16 was mixed with 125 μM $(TGACGT)^5$, which was labeled by Cy5, the band of free probe started to disappear (Fig. 6B). However, in these assays, clear shifted bands were not detected; instead, some smeared signals were apparent at the top part of the gels (Fig. 6B). In contrast, a band shift accompanied by a disappearance of free probe was clearly observed by mixing more than 5 μg mL^{-1} PtbZIP11 with 125 μM $(TGACGT)^5$ (Fig. 6B).

In order to confirm the binding specificity between CCRE motifs and PtbZIP11, additional gel-shift assays were carried out using nonlabeled competitor sequences. When 25 μg mL^{-1} PtbZIP11 was mixed with 125 μg mL^{-1} of either of the two types of CCRE pentamers, $(TGACGT/C)^5$, clear band shifts were observed (Fig. 6C). However, these shifted bands began to disappear with the addition of nonlabeled specific competitors for $(TGACGT)^5$ or $(TGACGC)^5$ at 10-fold higher concentrations for the labeled probe, and band shifts were completely abolished by the addition of 100-fold specific competitors (Fig. 6C). In sharp contrast, the addition of nonspecific competitor to concentrations 100-fold higher than the labeled probe did not inhibit the band shifts of either $(TGACGT)^5$ or $(TGACGC)^5$ (Fig. 6C).

Expression Profiles of *ptbZIP11* during Acclimation from High CO_2 to Air

Since the mode of regulation of P*ptca1* was demonstrated previously to be repression under high-CO_2 conditions mediated by cAMP and derepression under normal air conditions (Harada et al., 2006), PtbZIP11 is most likely to act as a repressor of transcription. The expression of *ptbZIP11* was analyzed during cell acclimation from 5% CO_2 to air by quantitative (q)PCR and was related to that of *ptca1* (Fig. 6D). It was apparent that *ptbZIP11* mRNA constitutively accumulated independently of ambient CO_2 concentrations (Fig. 6D), whereas that of *ptca1* was completely repressed in 5% CO_2 but was fully derepressed under air conditions (Fig. 6D). Transcript

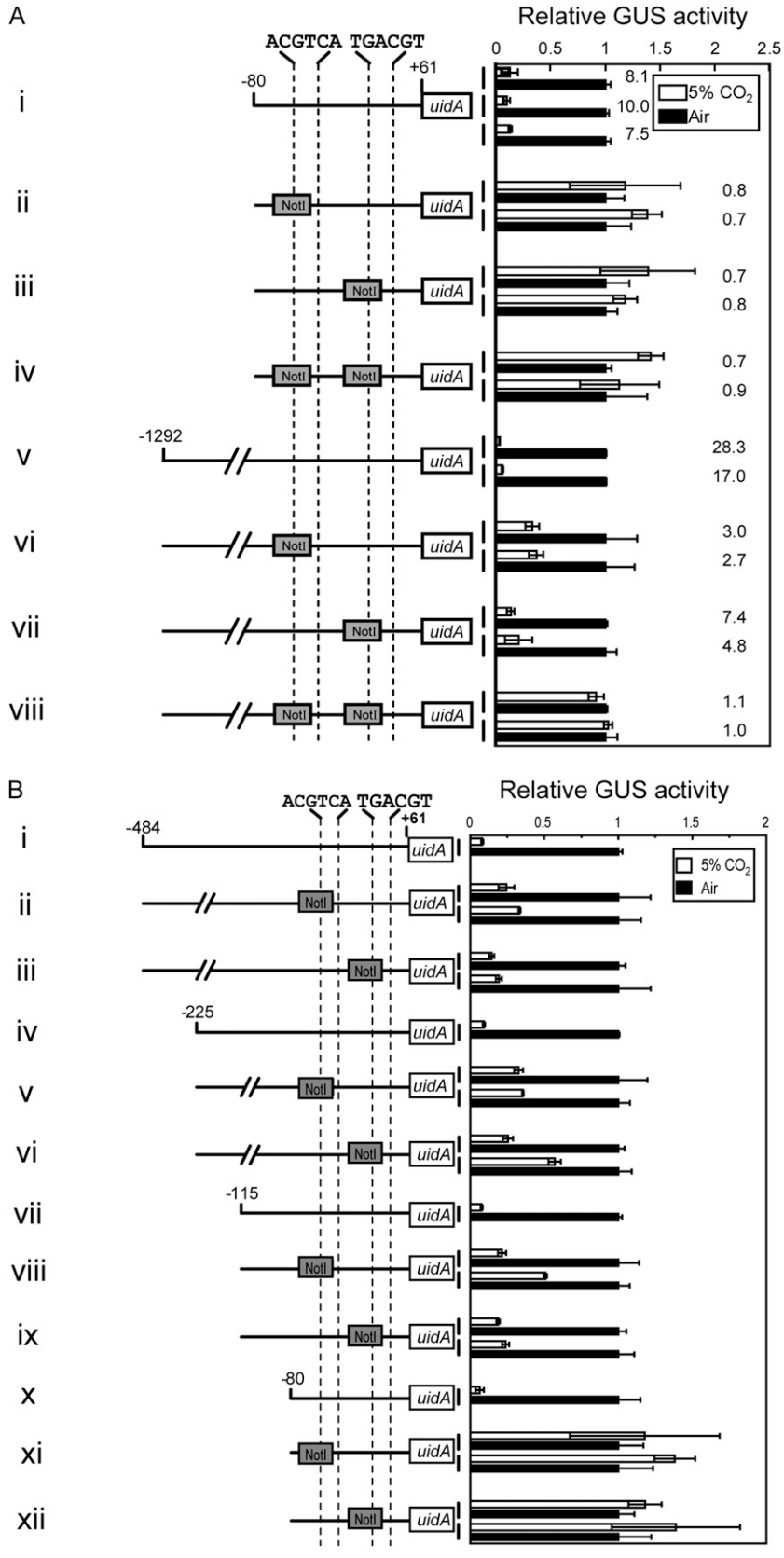

Figure 4. CO_2 response of P*ptca1* with an introduced *Not*I site within putative CO_2-responsive elements. A, Two different lengths of P*ptca1* (−80 to +61 and −1,292 to +61 relative to the transcription start site) were ligated to the *uidA* reporter gene in the pPha-T1 vector, and fragments of newly identified CO_2-responsive elements, ACGTCA and/or GTGACGC, were substituted with the *Not*I restriction site. GUS activities in lysates of each transformant grown in 5% CO_2 (white bars) are expressed as relative values to those in air-grown cells (black bars). GUS reporter assays were made on two to three clones obtained from each transformation. Values of each bar are means ± SD of three separate cultures. Ratios of GUS activity in air-grown cells to that in 5% CO_2-grown cells are shown to the right of the bars. B, The upstream truncated fragments (−484 to +61, −225 to +61, −115 to +61, and −80 to +61 relative to the transcription start site) of P*ptca1* were ligated to the *uidA* reporter gene in the pPha-T1 vector, and either the ACGTCA or GTGACGT motif was disrupted by the *Not*I restriction site. The intact promoter of each length is also shown as a control. GUS activities in lysates of each transformant grown in 5% CO_2 (white bars) are expressed as relative values to those in air-grown cells (black bars). GUS reporter assays were made on two to three clones obtained from each transformation. Values of each bar are means ± SD obtained from three separate cultures. Ratios of GUS activity in air-grown cells to that in 5% CO_2-grown cells are shown to the right of the bars.

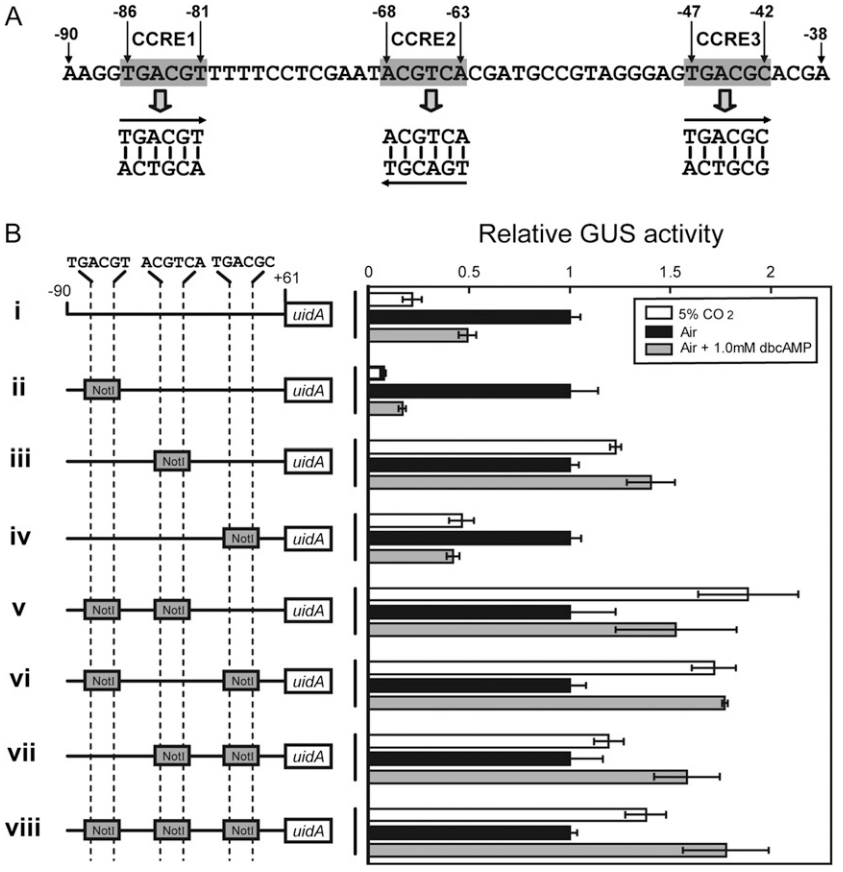

Figure 5. Primary structure of the putative core regulatory region of P*ptca1*, and confirmation of the function of three inverted repeats in the CO_2 and cAMP responsiveness of P*ptca1*. A, The three inverted sequences, TGACGT/C, newly found in P*ptca1*. B, The core regulatory region (−90 to +61 relative to the transcription start site) of P*ptca1* was ligated to the *uidA* reporter gene in the pPhaT1 vector, and parts or all three inverted sequences were substituted with the *Not*I restriction site with different combinations (left half). GUS activities in lysates of each transformant grown in 5% CO_2 (white bars) and acclimated to air in the presence of dbcAMP (gray bars) are expressed as relative values to those in air-grown cells (black bars). Values of each bar are means ± SD obtained from three separate cultures. Ratios of GUS activity in air-grown cells to that in 5% CO_2-grown cells are shown to the right of the bars.

levels of *ptbZIP11* were temporarily increased upon transfer of high-CO_2 cells to air, but levels under high CO_2 were equivalent to the basal air levels in cells acclimated for 12, 24, and 48 h (Fig. 6D). The relative expression level of *ptbZIP11* was about 2 orders of magnitude lower than that of *ptca1* in air-grown cells (Fig. 6D).

A Gain-of-Function Assay Using the CCRE Elements

In order to understand the topology of the putative transcription factors bound on the newly found CCRE elements to the basal transcriptional complex, a range of CCRE sequences were ligated to the minimal promoter (mP) of P*ptca1* (−10 to +61), and GUS reporter assays were carried out to assess the activity of the promoter. The distance between CCRE2 and mP was changed from 3 to 52 bp (Fig. 7, construct group a). The mP region alone drove GUS expression constitutively (Fig. 7, control). Interestingly, when CCRE2 was positioned immediately upstream (−3 bp) of mP, it conferred a clear CO_2 response on it (Fig. 7, construct group a, i). However, by extending the interval to 10 or 12 bp, CCRE2 became inert in conferring the CO_2 response (Fig. 7, construct group a, ii and iii), while the function was recovered again when the interval was further extended to between 14 and 22 bp (Fig. 7, construct group a, iv–vii). At distances greater than 32 bp, the effect of the single CCRE2 was lost completely (Fig. 7, construct group a, viii–x).

In contrast to the results for construct group a, vii to x, in which promoters partially or totally lost CO_2 responsiveness, CCRE2 at intervals 21, 31, 41, and 51 from mP showed a clear CO_2 response when CCRE3 was added downstream of CCRE2 (Fig. 7, construct group b, i–iv). Similarly, the presence of CCRE1 upstream of CCRE2 also increased the repressive activity of CCRE2 at longer intervals from mP (Fig. 7, construct group c). Notwithstanding, the promoters completely lost their CO_2 response in the absence of CCRE2 at any interval, even in the presence of both CCRE1 and CCRE3 (Fig. 7, construct group d). Raw activity data for Figure 7 are available in Supplemental Figure S4.

DISCUSSION

In our previous study, a repressive effect of both CO_2 and cAMP to P*ptca1* was clearly demonstrated both in qPCR assays of the endogenous *ptca1* transcript and in P*ptca1*::*uidA* reporter assays (Harada et al., 2006). This previous study also identified CRE1 and CRE2 and a putative p300be occurring downstream of −70 in P*ptca1*. Partial deletion of one of the CREs or the putative p300be resulted in derepression of P*ptca1* in high CO_2 or in the presence of dbcAMP in air. In this

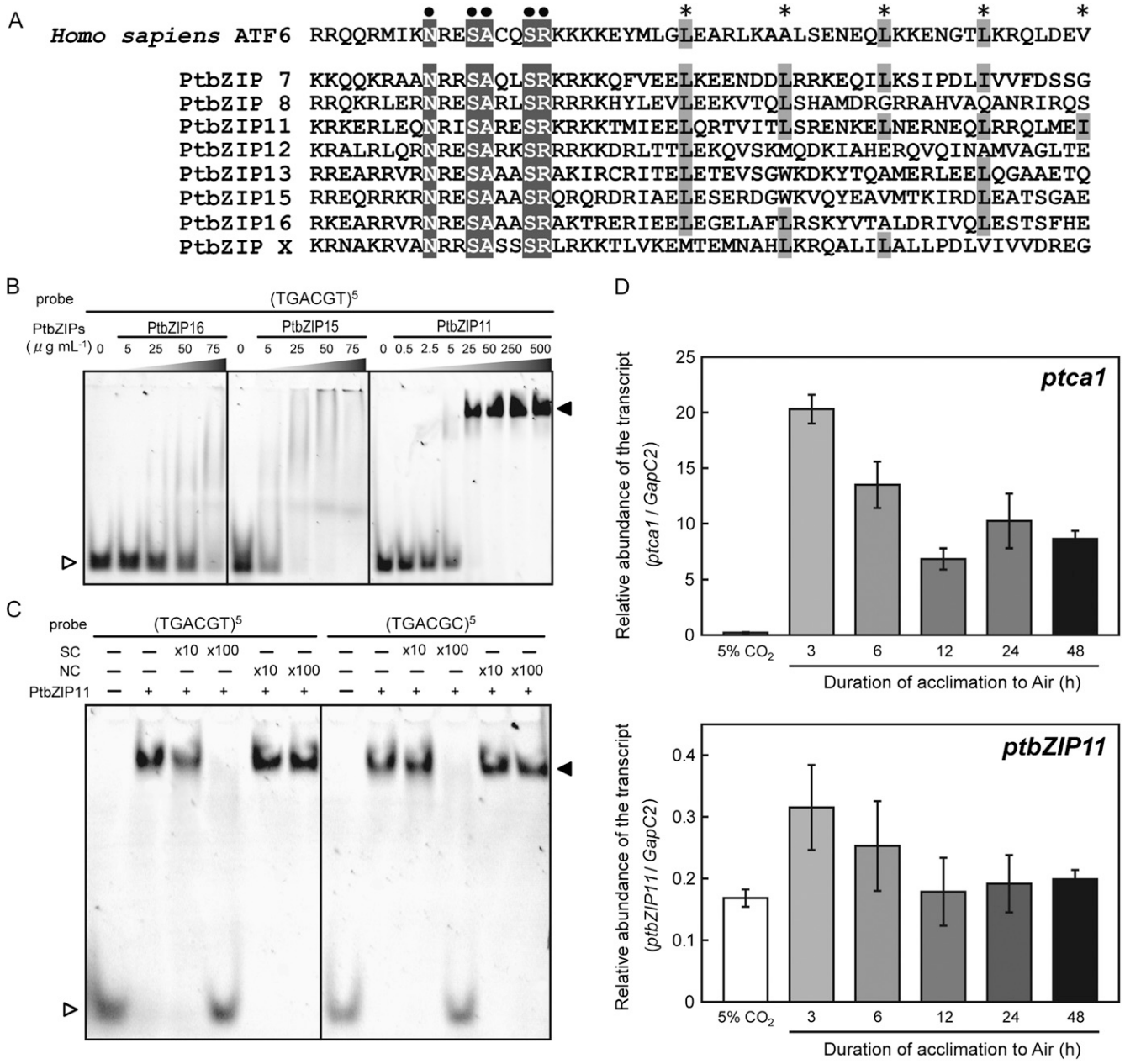

Figure 6. Structures, binding property to CCRE, and expression profile of putative human ATF6 superfamily transcription factors in *P. tricornutum*. A, Putative bZIP regions of eight candidates, which may belong to the human ATF6 superfamily (PtbZIP7, -8, -11, -12, -13, -15, -16, and -x), were aligned with that of the human ATF6 protein. The well-conserved DNA-binding sequences, which may target the CCRE motif, are indicated by black dots and highlighted. The putative repeats of Leu in the ZIP region are indicated by asterisks and highlighted. B, A concentration of 125 μM CCRE1 pentamer labeled by Cy5 was mixed with different concentrations of PtbZIP11, -15, and -16. The reactant was separated on 6% polyacrylamide gels, and bands were detected by fluorography. C, A concentration of 125 μM labeled CCRE1 or CCRE3 pentamer was mixed with 25 μg mL^{-1} PtbZIP11 in the absence or presence of competitors. A specific competitor (SC), which is the nonlabeled CCRE1 or CCRE3 pentamer, or a nonspecific competitor (NC), which is 5′-CGATTCAAATG-GAGAGTGGGTGAGCAAGGGCGAG-3′, was applied at concentrations 10 or 100 times more than the labeled probe. White and black arrowheads indicate free probe and shifted bands, respectively. D, qPCR of the *ptca1* and *ptbZIP11* transcripts was carried out on total RNAs extracted from cells grown in 5% CO_2, air, and cells acclimated from 5% CO_2 to air for 3, 6, 12, 24, and 48 h. Values are expressed as relative abundance to the amount of *Cytoplasmic Glyceraldehyde-3-Phosphate Dehydrogenase2* (*GapC2*) transcript.

study, the newly found elements, CCRE1 to CCRE3, were clearly shown to be CO_2-responsive elements that repressively control the transcription of *ptca1* in high-CO_2 conditions via the second messenger cAMP. We have further demonstrated that CCRE2 clearly overlapped with CRE1, but CCRE3 is new, since it did

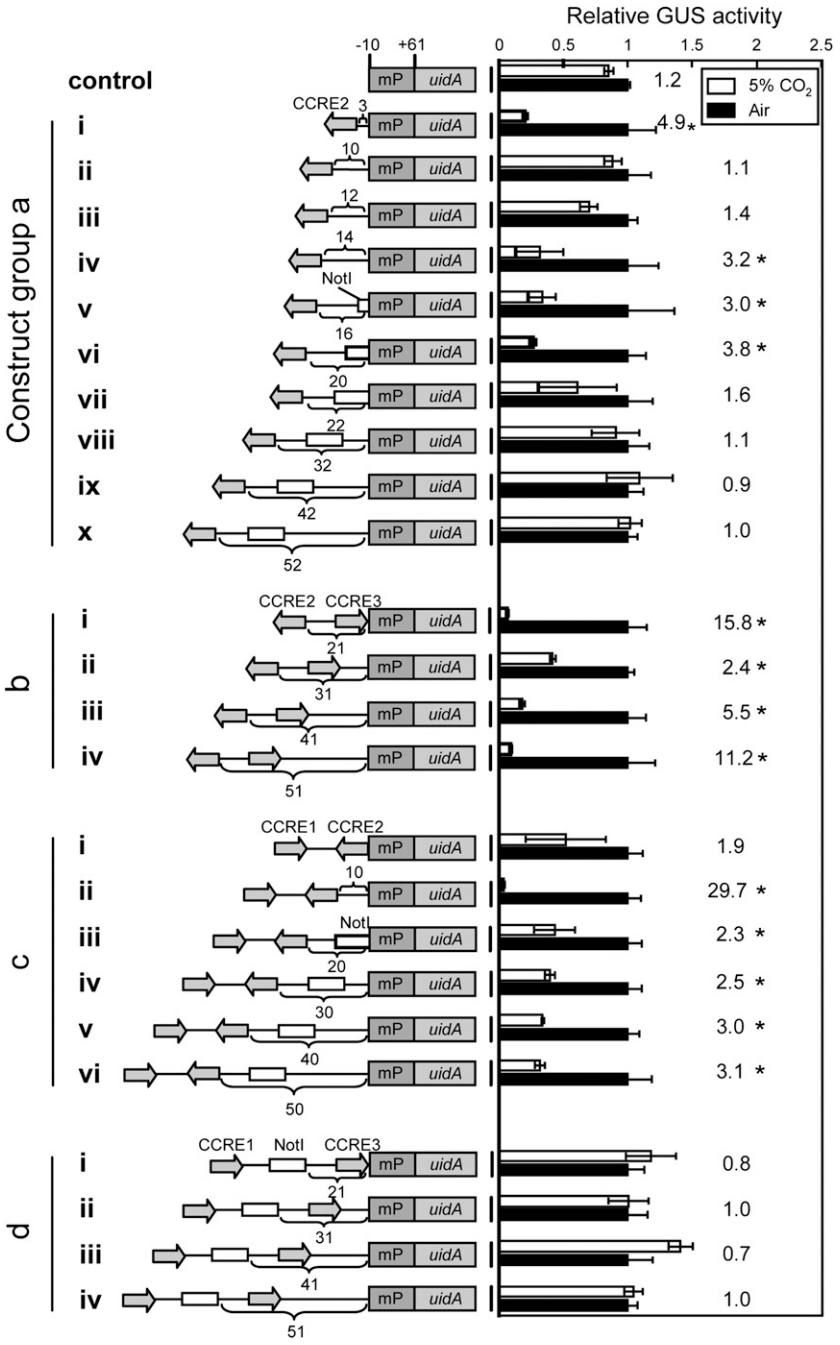

Figure 7. Gain-of-function assay using CCREs at altered distances from the mP region of P*ptca1*. The CCRE2 sequence was fused to mP of P*ptca1* (−10 to +61 relative to the transcription start site) at 10 different distances from 3 to 52 bp from mP (left half). GUS activities in lysates from each transformant grown in 5% CO_2 (white bars) are expressed as relative values to those in air-grown cells (black bars). Values of each bar are means ± SD obtained from three separate cultures. Ratios of GUS activity in air-grown cells to that in 5% CO_2-grown cells are shown to the right of the bars. Asterisks indicate ratios that exceed 2.0.

not match the putative p300be, which turned out no longer to be important. Skn-1 and CRE2 are also found to not be functional for CO_2 response in this study. The occurrence of CCRE1 was overlooked in the previous study due to an apparently sufficient repressive effect with only CCRE2 and CCRE3 in response to high CO_2 or dbcAMP. However, it was clearly shown in this study that CCRE1 complemented the absence of CCRE3.

CCRE1 to CCRE3 occurred with intervals of 12 to 15 nucleotides, which implies that each CCRE region locates by about two pitch turns of double-stranded DNA; thus, the plane of a base pair hybrid, which is targeted by a transcription factor, presumably faces to one side of the double helical structure of DNA in CCREs. CCRE2 is likely the most critical component among CCREs, due to its requirement for the CO_2 response of P*ptca1* (Fig. 5B).

It is interesting that CCRE1 and CCRE3 were nearly perfect inverted sequences of the CCRE2 element (Fig. 5A), strongly suggesting the pivotal requirement for CCRE2 to work cooperatively with CCRE1 and/or CCRE3. Synergistic effects between CRE-binding protein (CREB) and other transcription factors, which

target other cis-elements, have frequently been observed in cAMP-responsive transcriptional controls in mammalian cells (Hyman et al., 1989; Nitsch et al., 1993; Roesler et al., 1995). However, to our knowledge, the repression of a promoter by alternative combinations of three cAMP-responsive elements has not been observed previously.

In this study, eight genes presumably encoding putative transcription factors were retrieved in the genome database of *P. tricornutum*, based on the homology of bZIP domains to that of the human ATF6 family (Fig. 6A). These proteins showed a striking similarity in their putative DNA-binding domains, but sequences other than bZIP domains showed little similarity to each other or to any known sequences (Supplemental Fig. S1). It is thus suggested from the primary structure that these putative bZIP proteins could be categorized to the ATF6 superfamily, but their interaction partners and functions are likely to be unique to diatoms.

Structures and functions of ATF family proteins have been studied mostly in mammalian cells. In general, transcription-activating domains reside at their N termini, although the domain structures of the N-terminal regions are totally different depending on each ATF subclass (Rehfuss et al., 1991; Nomura et al., 1993; Ribeiro et al., 1994; van Dam et al., 1995; Haze et al., 1999; Hai and Hartman, 2001; Hashimoto et al., 2002). Most mammalian ATF family proteins have a bZIP domain at their C terminus, but ATF6, exceptionally, has a bZIP region within the central part of the sequence (Haze et al., 1999; Hai and Hartman, 2001). Human ATF6 is a transmembrane protein localized on the endoplasmic reticulum membrane and is transferred to the nucleus in response to endoplasmic reticulum stresses by proteolysis of both sides of the transmembrane domain by the proteases, S1P and S2P (Haze et al., 1999). PtbZIPs reported in this study also contained more central bZIP domains (Supplemental Fig. S1), although none of them possessed transmembrane regions, suggesting that their initial functional location in cells would also be unique to diatoms.

Recently, putative bZIP sequences were analyzed by Rayko et al. (2010) within the genomes of the two model diatoms, *P. tricornutum* and *Thalassiosira pseudonana*. Diatom bZIP sequences were divided into six groups and constituted a stramenopile-specific family, which showed no notable homology with those from other species (Rayko et al., 2010). ATF family candidates found in this study mainly belong to group 1 to 3 diatom bZIPs, although none of them (except PtbZIP7 and PtbZIPx) contained Per-Arnt-Sim domains. PtbZIPx could not be categorized into any of the subgroups reported by Rayko et al. (2010), but this putative transcription factor possesses a Per-Arnt-Sim domain overlapping with the bZIP domain (data not shown), strongly suggesting its relation to group 2 diatom bZIPs.

ATF family proteins form homodimers or heterodimers via their Leu-zipper domain upon binding to cis-elements (Hai and Curran, 1991; Liu et al., 2006). On the other hand, the number of Leu or Ile residues in putative Leu-zipper regions in PtbZIPs was variable, and some of the proteins, PtbZIP8, -12, -13, -15, and -x, may not even be able to form a dimer due to the lack of enough Leu repeats (Fig. 6A). Nonetheless, their DNA-binding motif is well conserved, strongly suggesting their function as transcription factors that are closely related to the bZIP family.

The binding and specificity of PtbZIP15 and -16 to $(TGACGT)^5$ were not clear (Fig. 6B), although an apparent decrease in free probe strongly suggested the affinity of these proteins to the element (Fig. 6B). Thus, PtbZIP11 is so far the only candidate transcription factor that directly binds to CCREs. However, from the results shown in Figure 6B, there is a possibility that other directly binding transcription factors besides PtbZIP11, which target CCREs with different affinities and may recruit different binding partners to CCRE regions, also participate in the regulatory system.

The constitutive expression under changing CO_2 conditions of the *ptbZIP11* transcription factor gene (Fig. 6D) strongly suggested that the function of PtbZIP11 is activated under high-CO_2 conditions by posttranslational processes in response to the increment of cytosolic cAMP. This is also the case for human ATF6, which is known to be expressed constitutively and whose function is regulated at the posttranslational level by proteolytic digestion (Haze et al., 1999). Accordingly, upon exposure of *P. tricornutum* cells to limited-CO_2 conditions, these repressive factors could be quickly deactivated by the reverse processes of the posttranscriptional modification to enable the derepression of P*ptca1* within 3 h (Fig. 6D).

The data from the gain-of-function assays strongly suggest that spatial configurations between transcription factors on CCRE2 and mP regions on the double helical strands of DNA critically control the affinity of the basal transcriptional complex on the mP region, and that CCRE1 or CCRE3 reveals a function to ensure this regulation only in the presence of CCRE2. In other words, when CCRE2 is close enough to the mP region, PtbZIPs on CCRE2 would stably immobilize the basal transcription complex or stabilize the repressor on mP and repress transcription (Fig. 8A), presumably mediated by some other transcription factors, which is conceptually depicted in Figure 8, as a mediator complex. But this system probably requires specific topology of these complexes on the DNA strands, which would be why repression was lost when CCRE2 was located on the twisted face of the DNA strand at relatively longer distances from mP (10–12 bp and more than 32 bp; Fig. 8B). The construct shown in Figure 7 (construct a, x) has the same distance between CCRE2 and mP as that in the intact P*ptca1*, but construct a, x, exhibited no repression. It is thus probable that, at distances greater than 10 to 12 bp, the DNA strand downstream of CCRE2 would need to bend to interact with the basal transcriptional complex, as demonstrated previously in NeP1 binding to the F1 silencer element of the chicken lysozyme gene (Arnold et al., 1996; Fig. 8C), and CCRE1 or CCRE3 may work

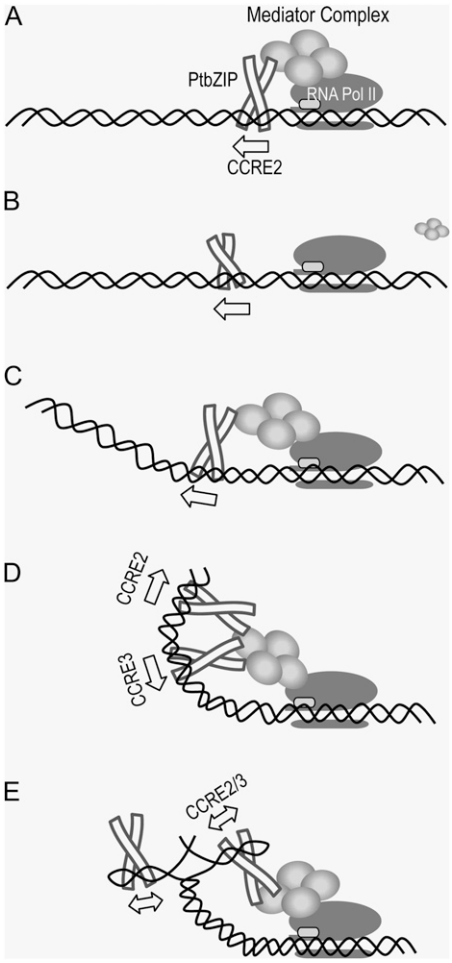

Figure 8. Speculative scheme showing repression models of P*ptca1* mediated by CCREs and the PtbZIP protein complex under high CO_2. A, In the gain-of-function analysis in Figure 7, direct harboring of a single CCRE2 to mP conferred a repression in high CO_2 (Fig. 7, construct a, i). The PtbZIP complex anchors into CCRE2 and immobilizes the basal transcription complex, presumably mediated by some repressive complex depicted as a mediator. B, Extension of the distance between mP and the single CCRE2 abolishes the repressive interaction (Fig. 7, construct a, ii and iii), presumably due to changes in the relative configuration between the PtbZIP complex and the basal transcription complex. C, The PtbZIP complex regains repression (Fig. 7, construct a, iv–vi) when it is turned back to the proper face of the DNA strand. The DNA strand needs to be bent at longer distances between CCRE2 and mP, which would be ensured by the strength of interaction between the PtbZIP complex, the putative repressive mediator, and the basal transcription complex. D and E, In the endogenous P*ptca1*, CCRE2 cooperates with either CCRE1 or CCRE3, which would ensure a stronger interaction with the basal transcription complex to be immobilized. Multiple PtbZIPs may strengthen the interaction (D), or a partial unfolding of the DNA strand at CCRE1/2 or CCRE2/3 may make the angle of the CCRE-PtbZIP complex pliable and ensure the interaction with the basal transcription complex (E). In the cartoons, the case of CCRE2 and CCRE3 is depicted.

with CCRE2 by stabilizing this DNA bending (Fig. 8D). This assumption is supported by the gain-of-function assays using construct groups b to d in Figure 7, which show that the repressive function of CCRE2 at locations longer than 32 bp from mP under high CO_2 was resumed when CCRE2 was combined with either CCRE1 or CCRE3.

CCREs are almost identical sequences that align in inverted directions within 50 bp of P*ptca1* (Fig. 5A). The functions of CCREs are likely specific for their directionality, because CCRE3 could not repress P*ptca1* even when the element was attached immediately upstream of mP in the absence of CCRE2 (Fig. 7, construct d, i). It is probable that the repression complex formed on CCREs would be asymmetric, whose function is thus highly dependent on the direction of the CCRE sequence. Such a direction-dependent complex should show its asymmetric property strongly when the location is artificially approximated to mP. In the intact P*ptca1*, CCREs need to work with alternative combinations of CCRE1/2 or CCRE2/3. Combination did not work between CCRE1 and CCRE3; thus, the partners probably need to be complementary with each other. According to the structural model of the CREB-CRE complex, a bZIP dimer occupies one CRE element (Schumacher et al., 2000). This is also presumed to be the case for PtbZIP11. Each of the two CCRE combinations would thus be expected to form two complexes of CCRE-PtbZIP11 on P*ptca1* (Fig. 8D). Alternatively, it is also possible that these combinations of CCREs form stem loops on each DNA strand when DNA is single stranded (Fig. 8E). However, epigenetic properties enabling such structural controls of P*ptca1* upon transcriptional switching still remain to be explored.

CONCLUSION

In this study, the precise sequences of CCREs in P*ptca1* and a possible transcription factor targeting them, PtbZIP11, were determined. Presumed topological models of P*ptca1* required for CO_2-cAMP-responsive transcription were proposed in this study, and the model suggested that a repeated number and directionality of CCREs (i.e. distances between CCREs and the relative location of CCREs from mP) are the critical factors in controlling P*ptca1* activity. Our preliminary study further found that other CO_2-responsive genes also possessed CCREs in their promoters but have different numbers and arrangements, and these promoters behave differently from CO_2 compared with that of P*ptca1* (Y. Matsuda, unpublished data). The model we propose in this study thus potentially provides an elemental example to understand the mechanisms of structural control of a promoter region, which lead to switching of transcriptional activity in response to changes in ambient CO_2 in marine diatoms.

MATERIALS AND METHODS

Cells and Culture Conditions

The marine diatom *Phaeodactylum tricornutum* (UTEX 642) was obtained from the University of Texas Culture Collection and was grown in artificial

seawater, which was supplemented with half-strength Guillard's "f" solution (F/2ASW; Guillard and Ryther, 1962; Harrison et al., 1980) under continuous illumination of 50 μmol m^{-2} s^{-1} photosynthetic photon flux density under constant aeration with 5% CO_2 or ambient air at 20°C. In acclimation experiments, 5% CO_2-grown cells were harvested by centrifugation at 3,500*g* for 5 min under room temperature, washed twice with CO_2-free F/2ASW, transferred to F/2ASW aerated with air, and allowed to acclimate for 1 to 2 d. In some experiments, 1.0 mM dbcAMP (Sigma-Aldrich) was added during the acclimation to air.

Preparation of Transformation Constructs

A series of upstream truncated constructs of P*ptca1* (−1,292 to +61, −484 to +61, −225 to +61, −115 to +61, −90 to +61, and −80 to +61 relative to the transcription start site) were amplified by PCR using P*ptca1* (−1,292 to +61) as a template. These constructs were phosphorylated and inserted into the blunt-ended site of transformation vector pFcpApGUS (Harada et al., 2005), which is a derivative of the general *P. tricornutum* transformation vector pPha-T1 equipped with a bleomycin-resistant gene cassette (Zaslavskaia et al., 2000).

A set of linker scan constructs with a *Not*I restriction site as the linker was synthesized by a modified inverse PCR method using the vector plasmid pFcpApGUS containing P*ptca1* (−80 to +61) as a template (Fig. 1A). Primer sets were designed to generate a *Not*I restriction site (gcggccgc) at desired locations by self-ligation (Fig. 1A). Fifteen linker-scan constructs −80 downstream from the transcription start site were generated (Fig. 1B, LS- and LS1–LS15).

In some experiments, *Not*I substitutions were introduced into −67 to −60 and/or −47 to −40 relative to the transcription start site using the aforementioned vector plasmid pFcpApGUS containing upstream truncated P*ptca1*s of five different lengths (−1,292 to +61, −484 to +61, −225 to +61, −115 to +61, and −80 to +61) as templates. In some experiments, *Not*I substitutions were introduced into −87 to −80, −69 to −62, and/or −48 to −41 relative to the transcription start site using the vector plasmid pFcpApGUS containing upstream truncated P*ptca1* (−90 to +61) as a template.

To generate one-base replacement constructs, PCR was carried out targeting the sequences −71 to −60 and −52 to −42 using the vector pFcpApGUS containing P*ptca1* (−80 to +61). To generate gain-of-function constructs for modeling P*ptca1* structure, LS7 was used as a template, and the distance between ACGTCA (−68 to −63) and mP was altered by a modified inverse PCR method. Primer sets were designed to alter the distance between ACGTCA and mP from 3 to 52 bp by self-ligation. Primer sequences used to generate these transformation constructs are summarized in Supplemental Table S7.

Transformation of *P. tricornutum*

Air-grown cells of *P. tricornutum* were harvested at midlogarithmic phase (optical density at 730 nm = 0.3–0.4). Approximately 5×10^7 cells were spotted as a plaque of 2.5 cm diameter on the surface of the F/2ASW agar plate. Five hundred micrograms of tungsten microcarrier (Bio-Rad; M17; approximately 1.1 μm particle size) was coated with 1.0 μg of plasmid DNA containing 1.0 M $CaCl_2$ and 16 mM spermidine. The PDS-1000/He Biolistic Particle Delivery System (Bio-Rad) was used for microprojectile bombardment of the microcarrier. The bombardment was done at 10.7 MPa to the cells in the chamber under negative pressure of 91.4 kPa with a target distance of 6 cm. Bombarded cells were maintained on the plate for 1 d in the dark and were then suspended in 2 mL of F/2ASW. This cell suspension was plated on agar plates containing 100 μg mL^{-1} Zeocin (Takara Bio) in F/2ASW and allowed to form colonies for 3 to 4 weeks under continuous illumination.

Screening of GUS-Expressing Transformants

Zeocin-resistant clones were suspended in 60 μL of GUS extraction buffer (50 mM sodium phosphate [pH 7.0], 10 mM β-mercaptoethanol, 0.1% [w/v] sodium lauryl sarcosine, and 0.1% [v/v] Triton X-100) containing 1 mM 5-bromo-4-chloro-3-indolyl-β-D-GlcA cyclohexyl ammonium salt (Sigma-Aldrich) on 96-well plates and were incubated overnight at 37°C. Transformants expressing GUS, which displayed the dark-blue-colored chromogenic reaction in the presence of 5-bromo-4-chloro-3-indolyl-β-D-GlcA cyclohexyl ammonium salt, were inoculated and used for further experiments.

Quantification of GUS Activity

Cells at different acclimation stages were harvested, disrupted by sonicator (Ultrasonic disruptor model UD-201; TOMY Seiko Co. Ltd.) in 0.5 to 1.0 mL of GUS extraction buffer (50 mM sodium phosphate [pH 7.0], 10 mM β-mercaptoethanol, and 0.1% [v/v] Triton X-100] in an ice bath, and then centrifuged at 15,000*g* for 5 min at 4°C. Lysate (18 μL) was added to 882 μL of GUS reaction buffer (10 mM *p*-nitrophenyl β-D-glucuronide in the GUS extraction buffer) and incubated at 37°C. The reaction was terminated by the addition of 0.5 M Na_2CO_3 every 10 min after starting the reaction, and the absorbance of *p*-nitrophenol released from the substrate was measured at 405 nm. Protein concentrations in lysate were measured by the Bradford method (Bio-Rad) according to the manufacturer's protocol.

Expression and Purification of PtbZIPs

Open reading frames of *ptbZIP*s were inserted into pET-21a vector designed to fuse the His hexamer to the C termini of products. Primer sets for the amplification of *ptbZIP*s are shown in Supplemental Table S6. PtbZIPs were expressed in *Escherichia coli* strain BL21(DE3) in 200 mL of Luria-Bertani medium supplemented with 1.0 mg mL^{-1} ampicillin and 0.5 mM isopropyl-1-thio-β-D-galactopyranoside. The *E. coli* cells were lysed by sonication in 10 mL of binding buffer (50 mM Tris-HCl [pH 8.0], 500 mM NaCl, and 5 mM imidazole). Crude lysates were applied to a 1-mL nickel-Sepharose column (Ni-Sepharose 6 Fast Flow; GE Healthcare Biosciences) repeatedly three times at 4°C, then washed with 12 mL of binding buffer (50 mM Tris-HCl [pH 8.0], 500 mM NaCl, and 5 mM imidazole) and 12 mL of washing buffer (50 mM Tris-HCl [pH 8.0], 500 mM NaCl, and 50 mM imidazole). After confirming the absorbance of eluate at 280 nm to be below 0.05, 12 mL of elution buffer (50 mM Tris-HCl [pH 8.0], 500 mM NaCl, and 300 mM imidazole) was applied to the column, and the eluates were collected for every 1 mL. The eluates were dialyzed with 1.2 L of imidazole-deprived buffer (50 mM Tris-HCl [pH 8.0] and 500 mM NaCl) using cellulose membranes (Viskase Companies). Concentrations of protein in eluate were determined by the Bradford method (Bio-Rad).

Gel-Shift Assay

As probes, pentamers of double-stranded 5′-TGACGT-3′ or 5′-TGACGC-3′ were labeled with Cy5 at their 5′ termini. A concentration of 2.5 mM labeled probe was added to 100 mL of annealing buffer (10 mM Tris-HCl [pH 7.5], 50 mM NaCl, and 5 mM EDTA), incubated at 96°C for 10 min, and then gradually cooled to 30°C for 45 min. The labeled probes at a final concentration of 125 μM were mixed with different concentrations of purified PtbZIPs in binding buffer (30 mM Tris-HCl [pH 7.5], 0.6 mM EDTA, 0.6 mM dithiothreitol, 50 mM KCl, 1 mM $MgCl_2$, and 12% glycerol) and incubated for 30 min at 20°C. In some experiments, 1.25 or 12.5 mM nonlabeled DNA probes, which have either the same sequence to labeled probes or noncompetitive sequence (5′-CGATTCAAATGGAGAGTGGGTGAGCAAGGGCGAG-3′) to the labeled probe, were added in the binding buffer. Samples were mixed with 3 μL of 50% glycerol, separated on a nondenaturing 6% polyacrylamide gel in 0.5× Tris-borate/EDTA, and Cy5 signal was observed by a fluorescence imager (Molecular Imager FX; Bio-Rad).

Quantification of *ptbZIP11* Transcript

Wild-type cells of *P. tricornutum* grown in 5% CO_2 or acclimated to air were harvested at midlogarithmic phase. Cells were pelleted by centrifugation and immediately frozen in liquid nitrogen. Total RNA was extracted from 5% CO_2-grown cells or cells acclimated to air for 3, 6, 12, 24, and 48 h using the RNeasy Plant Mini kit (Qiagen) according to the manufacturer's protocol. One microgram of total RNA was reverse transcribed with oligo$(dT)_{20}$ primer (Toyobo) and reverse transcriptase (Revertra Ace; Toyobo) to generate single-stranded cDNAs. The amount of PCR products was standardized by known amounts of template using plasmids containing full-length *ptbZIP11* (accession no. AB573061), *ptca1* (accession no. AF414191), or cytosolic glyceraldehyde-3-phosphate dehydrogenase gene (*GapC2*; accession no. AF063805), which were amplified respectively with the following sets of forward and reverse primers: PtbZIP7RTF (5′-CTTGCAAGCGATTGTGGGTC-3′) and PtbZIP7RTR (5′-CCAGGCCATGGGATTAAAGTTC-3′); PtCA1RTF (5′-TCACAATTCCTAGCAGAAAATCATCG-3′) and PtCA1RTR (5′-ACGCATCCAATGTACAAGTACTTGGG-3′); GapC2F (5′-TTTTTCGCCTTTCTAAACATCAGTT-3′) and GapC2R (5′-TACTCGGGCGTCAAGAAGG-3′). qPCR was carried out

using the Smart Cycler Thermal Cycler System (Cepheid) and SYBR Premix Ex Taq (Takara Bio) under PCR conditions as follows; for *ptbZIP11* and *ptca1*, heating at 95°C for 10 s, followed by 45 cycles of denaturing at 95°C for 5 s, annealing at 63°C for 20 s, and polymerase reaction at 72°C for 10 s; for *GapC2*, annealing temperature was 60°C. The amounts of cDNAs of *ptbZIP11* and *ptca1* were normalized as ratios to that of *GapC2*.

Sequence data from this article can be found in the GenBank/EMBL database under accession numbers as follows: *ptbZIP7* (AB573067), *ptbZIP8* (AB573064), *ptbZIP11* (AB573066), *ptbZIP12* (AB573065), *ptbZIP13* (AB573061), *ptbZIP15* (AB573063), *ptbZIP16* (AB573062), *ptbZIPx* (AB648938), *ptca1* (AF414191), *uidA* (S69414), and *Homo sapiens* ATF6 (AAB64434).

Supplemental Data

The following materials are available in the online version of this article.

Supplemental Figure S1. Sequence alignment of human ATF6 and eight PtbZIPs.

Supplemental Figure S2. Confirmation of the expression of PtbZIPs in *E. coli* strain BL21(DE3).

Supplemental Figure S3. Purification of PtbZIP11, -15, and -16 on a nickel-Sepharose column.

Supplemental Figure S4. Original activity data of GUS assays in Figures 3, 4, 5, and 7.

Supplemental Table S1. Primer sequences used to synthesize upstream truncated constructs.

Supplemental Table S2. Primer sequences used to synthesize linker-scan constructs.

Supplemental Table S3. Primer sequences used to synthesize one-base replacement constructs around CRE1.

Supplemental Table S4. Primer sequences used to synthesize one-base replacement constructs around p300be.

Supplemental Table S5. Primer sequences used for the insertion of the *Not*I sequence into CCREs.

Supplemental Table S6. Primer sequences for the amplification of *ptbZIPs*.

Supplemental Table S7. Primer sequences used to synthesize P*ptca1* modeling constructs.

ACKNOWLEDGMENTS

We thank Prof. Chris Bowler for critical reading of the manuscript, Mr. Atsushi Tanaka, Mr. Keiji Goto, and Ms. Nobuko Higashiuchi for their technical assistance, and Ms. Miyabi Inoue for her skillful secretarial aid.

Received October 29, 2011; accepted November 14, 2011; published November 17, 2011.

LITERATURE CITED

Arnold R, Burcin M, Kaiser B, Muller M, Renkawitz R (1996) DNA bending by the silencer protein NeP1 is modulated by TR and RXR. Nucleic Acids Res **24:** 2640–2647

Badger MR, Andrews TJ, Whitney SM, Ludwig M, Yellowlees DC, Leggat W, Price GD (1998) The diversity and co-evolution of Rubisco, plastids, pyrenoids and chloroplast-based CO_2-concentrating mechanisms in the algae. Can J Bot **76:** 1052–1071

Burkhardt S, Amoroso G, Riebesell U, Sültemeyer D (2001) CO_2 and HCO_3^- uptake in marine diatoms acclimated to different CO_2 concentrations. Limnol Oceanogr **46:** 1378–1391

Cann MJ, Hammer A, Zhou J, Kanacher T (2003) A defined subset of adenylyl cyclases is regulated by bicarbonate ion. J Biol Chem **278:** 35033–35038

Chen X, Qiu CE, Shao JZ (2006) Evidence for K^+-dependent HCO_3^- utilization in the marine diatom *Phaeodactylum tricornutum*. Plant Physiol **141:** 731–736

Chen Y, Cann MJ, Litvin TN, Iourgenko V, Sinclair ML, Levin LR, Buck J (2000) Soluble adenylyl cyclase as an evolutionarily conserved bicarbonate sensor. Science **289:** 625–628

Colman B, Huertas E, Bhatti S, Dason JS (2002) The diversity of inorganic carbon acquisition mechanisms in eukaryotic microalgae. Funct Plant Biol **29:** 261–270

Colman B, Rotatore C (1995) Photosynthetic inorganic carbon uptake and accumulation in two marine diatoms. Plant Cell Environ **18:** 919–924

Deutsch PJ, Hoeffler JP, Jameson JL, Lin JC, Habener JF (1988) Structural determinants for transcriptional activation by cAMP-responsive DNA elements. J Biol Chem **263:** 18466–18472

Eriksson M, Villand P, Gardeström P, Samuelsson G (1998) Induction and regulation of expression of a low-CO_2-induced mitochondrial carbonic anhydrase in *Chlamydomonas reinhardtii*. Plant Physiol **116:** 637–641

Falkowski P, Scholes RJ, Boyle E, Canadell J, Canfield D, Elser J, Gruber N, Hibbard K, Högberg P, Linder S, et al (2000) The global carbon cycle: a test of our knowledge of earth as a system. Science **290:** 291–296

Fujiwara S, Fukuzawa H, Tachiki A, Miyachi S (1990) Structure and differential expression of two genes encoding carbonic anhydrase in *Chlamydomonas reinhardtii*. Proc Natl Acad Sci USA **87:** 9779–9783

Fukuzawa H, Miura K, Ishizaki K, Kucho KI, Saito T, Kohinata T, Ohyama K (2001) Ccm1, a regulatory gene controlling the induction of a carbon-concentrating mechanism in Chlamydomonas reinhardtii by sensing CO_2 availability. Proc Natl Acad Sci USA **98:** 5347–5352

Guillard RRL, Ryther JH (1962) Studies of marine planktonic diatoms. I. *Cyclotella nana* Hustedt, and *Detonula confervacea* (cleve) Gran. Can J Microbiol **8:** 229–239

Hai T, Curran T (1991) Cross-family dimerization of transcription factors Fos/Jun and ATF/CREB alters DNA binding specificity. Proc Natl Acad Sci USA **88:** 3720–3724

Hai T, Hartman MG (2001) The molecular biology and nomenclature of the activating transcription factor/cAMP responsive element binding family of transcription factors: activating transcription factor proteins and homeostasis. Gene **273:** 1–11

Hammer A, Hodgson DRW, Cann MJ (2006) Regulation of prokaryotic adenylyl cyclases by CO_2. Biochem J **396:** 215–218

Harada H, Matsuda Y (2005) Identification and characterization of a new carbonic anhydrase in the marine diatom *Phaeodactylum tricornutum*. Can J Bot **83:** 909–916

Harada H, Nakajima K, Sakaue K, Matsuda Y (2006) CO_2 sensing at ocean surface mediated by cAMP in a marine diatom. Plant Physiol **142:** 1318–1328

Harada H, Nakatsuma D, Ishida M, Matsuda Y (2005) Regulation of the expression of intracellular β-carbonic anhydrase in response to CO_2 and light in the marine diatom *Phaeodactylum tricornutum*. Plant Physiol **139:** 1041–1050

Harrison PJ, Waters RE, Taylor FJR (1980) A broad spectrum artificial seawater medium for coastal and open ocean phytoplankton. J Phycol **16:** 28–35

Hashimoto Y, Zhang C, Kawauchi J, Imoto I, Adachi MT, Inazawa J, Amagasa T, Hai T, Kitajima S (2002) An alternatively spliced isoform of transcriptional repressor ATF3 and its induction by stress stimuli. Nucleic Acids Res **30:** 2398–2406

Haze K, Yoshida H, Yanagi H, Yura T, Mori K (1999) Mammalian transcription factor ATF6 is synthesized as a transmembrane protein and activated by proteolysis in response to endoplasmic reticulum stress. Mol Biol Cell **10:** 3787–3799

Hyman SE, Comb M, Pearlberg J, Goodman HM (1989) An AP-2 element acts synergistically with the cyclic AMP- and phorbol ester-inducible enhancer of the human proenkephalin gene. Mol Cell Biol **9:** 321–324

Johnston AM, Raven JA (1996) Inorganic carbon accumulation by the marine diatom *Phaeodactylum tricornutum*. Eur J Phycol **31:** 285–290

Kaplan A, Badger MR, Berry JA (1980) Photosynthesis and intracellular inorganic carbon pool in the blue green alga *Anabaena variabilis*: response to external CO_2 concentration. Planta **149:** 219–226

Kitao Y, Matsuda Y (2009) Formation of macromolecular complexes of carbonic anhydrases in the chloroplast of a marine diatom by the action of the C-terminal helix. Biochem J **419:** 681–688

Klengel T, Liang WJ, Chaloupka J, Ruoff C, Schröppel K, Naglik JR, Eckert SE, Mogensen EG, Haynes K, Tuite MF, et al (2005) Fungal

adenylyl cyclase integrates CO_2 sensing with cAMP signaling and virulence. Curr Biol **15:** 2021–2026

Kucho K, Yoshioka S, Taniguchi F, Ohyama K, Fukuzawa H (2003) Cis-acting elements and DNA-binding proteins involved in CO_2-responsive transcriptional activation of Cah1 encoding a periplasmic carbonic anhydrase in *Chlamydomonas reinhardtii*. Plant Physiol **133:** 783–793

Liu H, Deng X, Shyu YJ, Li JJ, Taparowsky EJ, Hu CD (2006) Mutual regulation of c-Jun and ATF2 by transcriptional activation and subcellular localization. EMBO J **25:** 1058–1069

Matsuda Y, Colman B (1995) Induction of CO_2 and bicarbonate transport in the green alga *Chlorella ellipsoidea*: time course of induction of the two systems. Plant Physiol **108:** 247–252

Matsuda Y, Hara T, Colman B (2001) Regulation of the induction of bicarbonate uptake by dissolved CO_2 in the marine diatom, *Phaeodactylum tricornutum*. Plant Cell Environ **24:** 611–620

Matsuda Y, Nakajima K, Tachibana M (2011) Recent progresses on the genetic basis of the regulation of CO_2 acquisition systems in response to CO_2 concentration. Photosynth Res **109:** 191–203

Miller AG, Espie GS, Canvin DT (1990) Physiological aspects of CO_2 and HCO_3^- transport by cyanobacteria: a review. Can J Bot **68:** 1291–1302

Montminy MR, Sevarino KA, Wagner JA, Mandel G, Goodman RH (1986) Identification of a cyclic-AMP-responsive element within the rat somatostatin gene. Proc Natl Acad Sci USA **83:** 6682–6686

Moroney JV, Ynalvez RA (2007) Proposed carbon dioxide concentrating mechanism in Chlamydomonas reinhardtii. Eukaryot Cell **6:** 1251–1259

Nishimura T, Takahashi Y, Yamaguchi O, Suzuki H, Maeda S, Omata T (2008) Mechanism of low CO_2-induced activation of the *cmp* bicarbonate transporter operon by a LysR family protein in the cyanobacterium *Synechococcus elongatus* strain PCC 7942. Mol Microbiol **68:** 98–109

Nitsch D, Boshart M, Schütz G (1993) Activation of the tyrosine aminotransferase gene is dependent on synergy between liver-specific and hormone-responsive elements. Proc Natl Acad Sci USA **90:** 5479–5483

Nomura N, Zu YL, Maekawa T, Tabata S, Akiyama T, Ishii S (1993) Isolation and characterization of a novel member of the gene family encoding the cAMP response element-binding protein CRE-BP1. J Biol Chem **268:** 4259–4266

Omata T, Gohta S, Takahashi Y, Harano Y, Maeda S (2001) Involvement of a CbbR homolog in low CO_2-induced activation of the bicarbonate transporter operon in cyanobacteria. J Bacteriol **183:** 1891–1898

Price GD, Badger MR, Woodger FJ, Long BM (2008) Advances in understanding the cyanobacterial CO_2-concentrating-mechanism (CCM): functional components, Ci transporters, diversity, genetic regulation and prospects for engineering into plants. J Exp Bot **59:** 1441–1461

Rayko E, Maumus F, Maheswari U, Jabbari K, Bowler C (2010) Transcription factor families inferred from genome sequences of photosynthetic stramenopiles. New Phytol **188:** 52–66

Rehfuss RP, Walton KM, Loriaux MM, Goodman RH (1991) The cAMP-regulated enhancer-binding protein ATF-1 activates transcription in response to cAMP-dependent protein kinase A. J Biol Chem **266:** 18431–18434

Reinfelder JR, Milligan AJ, Morel FMM (2004) The role of the C_4 pathway in carbon accumulation and fixation in a marine diatom. Plant Physiol **135:** 2106–2111

Ribeiro A, Brown A, Lee KAW (1994) An *in vivo* assay for members of the cAMP response element-binding protein family of transcription factors. J Biol Chem **269:** 31124–31128

Rikitake Y, Moran E (1992) DNA-binding properties of the E1A-associated 300-kilodalton protein. Mol Cell Biol **12:** 2826–2836

Roberts K, Granum E, Leegood RC, Raven JA (2007) C3 and C4 pathways of photosynthetic carbon assimilation in marine diatoms are under genetic, not environmental, control. Plant Physiol **145:** 230–235

Roesler WJ, Graham JG, Kolen R, Klemm DJ, McFie PJ (1995) The cAMP response element binding protein synergizes with other transcription factors to mediate cAMP responsiveness. J Biol Chem **270:** 8225–8232

Rotatore C, Colman B (1992) Active uptake of CO_2 by the diatom *Navicula pelliculosa*. J Exp Bot **43:** 571–576

Satoh D, Hiraoka Y, Colman B, Matsuda Y (2001) Physiological and molecular biological characterization of intracellular carbonic anhydrase from the marine diatom *Phaeodactylum tricornutum*. Plant Physiol **126:** 1459–1470

Schumacher MA, Goodman RH, Brennan RG (2000) The structure of a CREB bZIP.somatostatin CRE complex reveals the basis for selective dimerization and divalent cation-enhanced DNA binding. J Biol Chem **275:** 35242–35247

Spalding MH (2008) Microalgal carbon-dioxide-concentrating mechanisms: *Chlamydomonas* inorganic carbon transporters. J Exp Bot **59:** 1463–1473

Sültemeyer D (1998) Carbonic anhydrase in eukaryotic algae: characterization, regulation, and possible function during photosynthesis. Can J Bot **76:** 962–972

Tachibana M, Allen AE, Kikutani S, Endo Y, Bowler C, Matsuda Y (2011) Localization of putative carbonic anhydrases in two marine diatoms, *Phaeodactylum tricornutum* and *Thalassiosira pseudonana*. Photosynth Res **109:** 205–221

Tanaka Y, Nakatsuma D, Harada H, Ishida M, Matsuda Y (2005) Localization of soluble β-carbonic anhydrase in the marine diatom *Phaeodactylum tricornutum*: sorting to the chloroplast and cluster formation on the girdle lamellae. Plant Physiol **138:** 207–217

Tanaka Y, Naruse I, Maekawa T, Masuya H, Shiroishi T, Ishii S (1997) Abnormal skeletal patterning in embryos lacking a single *Cbp* allele: a partial similarity with Rubinstein-Taybi syndrome. Proc Natl Acad Sci USA **94:** 10215–10220

Thoms S, Pahlow M, Gladrow DAW (2001) Model of the carbon concentrating mechanism in chloroplasts of eukaryotic algae. J Theor Biol **208:** 295–313

Tréguer P, Nelson DM, Van Bennekom AJ, Demaster DJ, Leynaert A, Quéguiner B (1995) The silica balance in the world ocean: a reestimate. Science **268:** 375–379

Trimborn S, Lundholm N, Thoms S, Richter KU, Krock B, Hansen PJ, Rost B (2008) Inorganic carbon acquisition in potentially toxic and non-toxic diatoms: the effect of pH-induced changes in seawater carbonate chemistry. Physiol Plant **133:** 92–105

Vance P, Spalding MH (2005) Growth, photosynthesis and gene expression in *Chlamydomonas* over a range of CO_2 concentrations and CO_2/O_2 ratios: CO_2 regulates multiple acclimation states. Can J Bot **83:** 796–809

van Dam H, Wilhelm D, Herr I, Steffen A, Herrlich P, Angel P (1995) ATF-2 is preferentially activated by stress-activated protein kinases to mediate c-*jun* induction in response to genotoxic agents. EMBO J **14:** 1798–1811

Vinson C, Myakishev M, Acharya A, Mir AA, Moll JR, Bonovich M (2002) Classification of human B-ZIP proteins based on dimerization properties. Mol Cell Biol **22:** 6321–6335

Walker AK, See R, Batchelder C, Kophengnavong T, Gronniger JT, Shi Y, Blackwell TK (2000) A conserved transcription motif suggesting functional parallels between *Caenorhabditis elegans* SKN-1 and Cap'n'Collar-related basic leucine zipper proteins. J Biol Chem **275:** 22166–22171

Wang HL, Postier BL, Burnap RL (2004) Alterations in global patterns of gene expression in *Synechocystis* sp. PCC 6803 in response to inorganic carbon limitation and the inactivation of ndhR, a LysR family regulator. J Biol Chem **279:** 5739–5751

Wang Y, Shen J, Arenzana N, Tirasophon W, Kaufman RJ, Prywes R (2000) Activation of ATF6 and an ATF6 DNA binding site by the endoplasmic reticulum stress response. J Biol Chem **275:** 27013–27020

Yoshioka S, Taniguchi F, Miura K, Inoue T, Yamano T, Fukuzawa H (2004) The novel Myb transcription factor LCR1 regulates the CO_2-responsive gene *Cah1*, encoding a periplasmic carbonic anhydrase in *Chlamydomonas reinhardtii*. Plant Cell **16:** 1466–1477

Xiang Y, Zhang J, Weeks DP (2001) The Cia5 gene controls formation of the carbon concentrating mechanism in Chlamydomonas reinhardtii. Proc Natl Acad Sci USA **98:** 5341–5346

Zaslavskaia LA, Lippmeier JC, Kroth PG, Grossman AR, Apt KE (2000) Transformation of the diatom *Phaeodactylum tricornutum* (Bacillariophyceae) with a variety of selectable marker and reporter genes. J Phycol **36:** 379–386